EMF PENETRATION IN BIOLOGICAL TISSUE WHEN EXPOSED IN THE NEAR FIELD OF A MOBILE PHONE ANTENNA

Mihaela Morega, Alina Machedon

POLITEHNICA University of Bucharest, mihaela@iem.pub.ro

Abstract. *The paper presents a numerical finite element (FEM) analysis of the electromagnetic field (EMF) penetration in structures that represent estimates of human anatomical tissues, in specific conditions associated to mobile phone technology. A 2D FEM models is created, where the human head is exposed in the microwaves (MW) frequency range used in mobile telephony (0.6 - 3 GHz), in the near field of dipole and monopole antennas. Numerical estimates of the Specific (energy) Absorption Rate (SAR) and electric field strength (E) inside the anatomical tissues are compared for different frequencies and exposure conditions. The results reveal the existence of SAR hot spots inside the head, particularly in the ear region.*

The objective of this work is to estimate EMF human exposure conditions in circumstances specific to the mobile telephony technology. For this purpose it was necessary to formulate and validate a 2D FEM model which represents an optimized compromise between the accuracy of the physical representation and the economy of the computational resources. The characteristics of the idealized 2D FEM model could be used for the design of simplified 3D FEM models and experimental phantoms.

INTRODUCTION

EMF produced by an antenna can be described as having several components. Only one of these actually propagates through space. This component is called the *radiated field* or *the far field*. The strength of the radiated field does decrease with distance, since the energy must spread as it travels. The other components of the electromagnetic field remain near the antenna and do not propagate. There are generally two other components: the static field and the induction field; their strength decreases very rapidly with distance. The entire field—all of the components—near the antenna is called the *near field*. In this region, approximately one wavelength in extent, the electric field strength can be relatively high and pose a hazard to the human body.

Localized human exposure to EMF in MW frequency range is associated to the use of mobile telephony, detection and positioning systems, dielectric heaters and to several medical procedures (hyperthermia in tumor therapy, neuronal implant growth, imaging techniques, etc.). Biomedical research in this field is based on the analysis of EMF interactions with body tissues and on epidemiological studies. In dosimetric estimates it is a scientific consensus to consider, in MW exposure, that thermal effects prevail and the *SAR* is the quantity that represents the "dose". At a macroscopic scale, *SAR* [W/kg] is defined as the absorbed power per unit mass at infinitesimal volume of tissue ($SAR = \sigma E^2/\rho$, where E is the rms value of the electric field strength, σ is the electric conductivity and ρ is the mass density of the tissue). *SAR* distribution depends on several factors: the incident field parameters (near or far field), geometric parameters (shape and structure) of the exposed body, dielectric properties of the tissues (as lossy dielectrics), ground/screen/reflector effects of other objects in the field near the body. The usefulness of numerical modeling as well as measurements of *SAR* and *E* inside the body has been demonstrated in the assessment of biological effects and in setting the

safety exposure guidelines and the certification protocols for harmless MW devices used in medicine, transportation and communication systems, and in day-to-day life.

The computational analysis is based on wave equations derived from Maxwell's equations. Calculations can be performed either by analytical [1] or by numerical methods [2], [3], [4]. Early works were done by theoretical analyses assuming a simple model, followed by more detailed models treated by numerical techniques [2]. Method of moments (MoM) [4] or the finite-difference time-domain (FDTD) method [3], [4] made an epoch in this field. The finite element method (FEM) works on adaptive meshes, better suited for heterogeneous media [5], [8]. Our paper presents a FEM based analysis of the human head exposure in the *near field* of an antenna.

FEM MODEL FOR THE EMF *NEAR FIELD* STUDY

The need for a reliable computational model in MW dosimetry related to mobile phone technology led us to try several approaches to simulate the human head and the EMF source [7], [8]. It is of common practice to generate simplified 3D models of the human head, in a spherical or elliptical layered structure [1], [4], as fig. 1 suggests. However, the realistic representation in 3D requires high computational resources. This is the main reason that sustains the simplified 2D model we have created. It is based on the geometry suggested in fig. 1.b, which is an ensemble of tissue layers; the 2D model results from the axial symmetry (around the longitudinal axis of the antenna) of a fictive anatomical structure. Even if, at the first glance, the original 3D geometry looks unrealistic, the 2D model proves its usefulness and performance by comparison with 3D models presented in the literature.

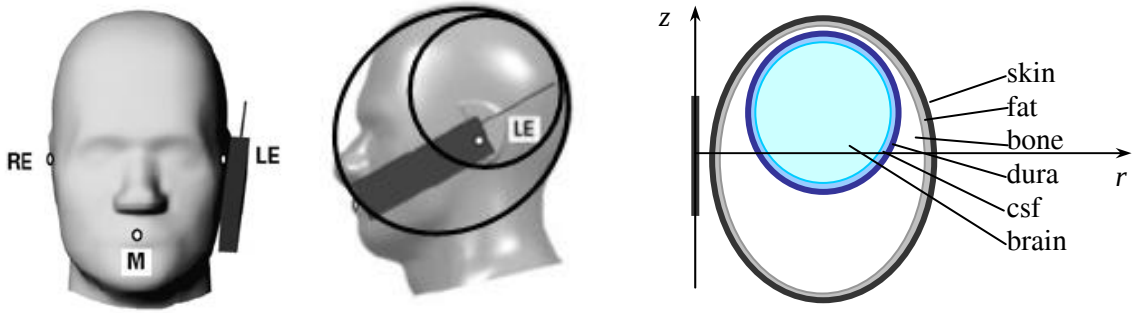

a. Characteristic position of the mobile phone **b.** Inner head structure

Fig. 1 Computational domain based on a multi-layered structure

The interaction of the time-harmonic EMF and human body at microwave frequencies is usually described in terms of the *complex permittivity* $\underline{\varepsilon} = \varepsilon - j\sigma/\omega$, or the *complex conductivity* $\underline{\sigma} = \sigma + j\omega\varepsilon$, where ε is the dielectric permittivity, σ is the electric conductivity and $\omega = 2\pi f$ is the angular frequency of the EMF. The biological tissues in this frequency range act as conductive (lossy) dielectric materials. The magnetic permeability is considered $\mu_0 = 4\pi 10^{-7}$ H/m. In addition to the electric properties, the *SAR* estimate requires the value of the mass density ρ, for each type of tissue. The specific values for σ, ε and ρ considered in our study correspond to data in literature [1], [6], [10]. For illustration, fig. 2 shows the frequency dependence of the electric conductivity σ and relative dielectric permittivity ε, for the six tissues involved (skin, fat, bone, dura, cerebro spinal fluid and brain) in the range used by the GSM mobile phone system.

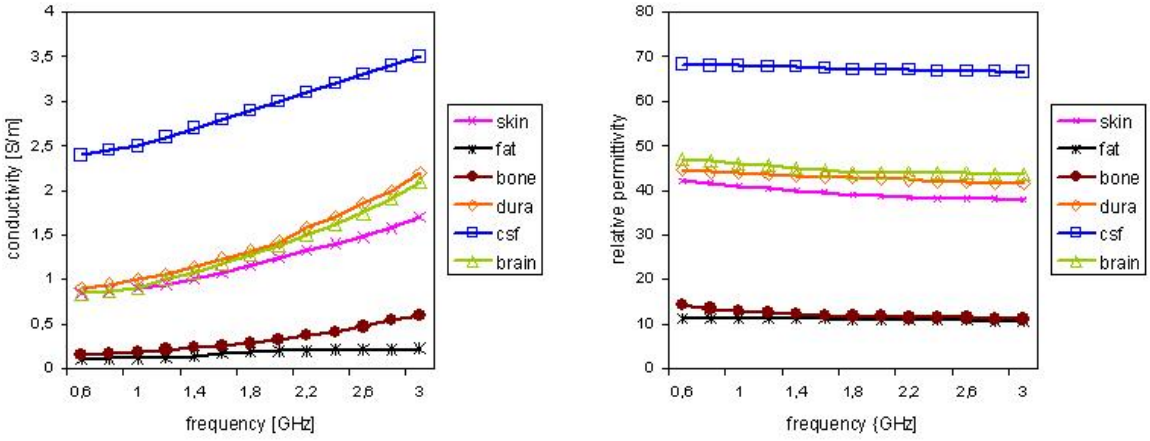

Fig. 2 Frequency dependence of the conductivity and the permittivity of several tissues, in the GSM frequency range

The EMF source is first considered a center fed half-wavelength dipole antenna, and then replaced by a quarter wavelength monopole antenna fed at its base. The characteristic dimension of the antenna, oriented on the (*oz*) axis, is accorded with the wavelength in the microwave frequency range used in European GSM mobile system telephony (0.6 – 3) GHz. The dipole antenna is placed symmetrically with regard to the (*or*) axis and the monopole antenna has its base (feeding point) in the origin of the axes. The user is exposed (with the head and ear) at a distance of 5 mm, in the near-field of the antenna [6].

The numerical computation used for the 2D FEM model is based on the FEMLAB software [11], the *Electromagnetics Module*, in the *axisymmetric transversal magnetic (TM) waves* application mode, *time-harmonic* submode. The wave equations are applied for lossy media, characterized by the complex electric permittivity $\underline{\varepsilon}$

$$\nabla\times\left(\frac{1}{\mu_0}\nabla\times\underline{\mathbf{E}}\right)-\omega^2\underline{\varepsilon}\underline{\mathbf{E}}=0\,,\qquad \nabla\times\left(\frac{1}{\underline{\varepsilon}}\nabla\times\underline{\mathbf{H}}\right)-\omega^2\mu_0\underline{\mathbf{H}}=0\,, \tag{1}$$

where the unknown field variables, in the cylindrical coordinate system and in complex form are:

$$\underline{\mathbf{H}}(r,z,t)=\underline{H}_\varphi(r,z)\mathbf{e}_\varphi e^{j\omega t}\,,\qquad \underline{\mathbf{E}}(r,z,t)=\left(\underline{E}_r(r,z)\mathbf{e}_r+\underline{E}_z(r,z)\mathbf{e}_z\right)e^{j\omega t}\,. \tag{2}$$

The computational domain is limited with *low-reflecting* boundary conditions

$$\mathbf{n}\times\left(\frac{\underline{\varepsilon}}{\mu_0}\right)^{1/2}\underline{\mathbf{E}}-H_\varphi=-2H_{\varphi 0}\,,\quad H_{\varphi 0}=0\,, \tag{3}$$

and the boundary on the (*Oz*) axis satisfies *axial symmetry* conditions

$$E_r=0\,,\quad \frac{\partial E_z}{\partial r}=0\,,\quad \frac{\partial H_\varphi}{\partial z}=0\,,\quad \frac{1}{r}\frac{\partial H_\varphi}{\partial r}-\frac{1}{r^2}H_\varphi=0\,. \tag{4}$$

The EMF source is introduced through a nonhomogeneous *magnetic field* boundary condition, simulating the center fed dipole antenna, respectively the base fed monopole

antenna. The magnetic field condition is adjusted each time, so that the emitted power is constant (125 mW) in all studied cases.

The FEMLAB linear stationary solver based on Gaussian elimination was applied. The FEM mesh is composed of triangular elements, and two types of accuracy tests were performed for its assessment: the constant radiated power and an energetic balance (the radiated power compared with the sum of the power absorbed in the body and the power radiated in the far field). A FEM mesh with aprox. 40000 nodes and 60000 elements was currently adopted in our computations.

VALIDATION OF THE 2D FEM MODEL

A set of numerical tests was conducted to validate the **2D FEM model**, based on the axial symmetry described earlier. We have generated two similar test models; each of them is inspired by the structure of a 3D spherical layered model, published in literature; our results are compared with those published, in order to validate our simplified 2D FEM models.

Test model nr. 1 has a circular multi-layered structure, with six different tissues: skin, fat, bone, dura, cerebro-spinal fluid (csf) and brain. The 2D axisymmetric computational domain (in *rOz* plane) looks similar to the plane section (*xOy*) of the spherical domain described in [1] (fig. 3). Table 1 gives the values of the electric properties, mass densities and dimensions for the subdomains [1].

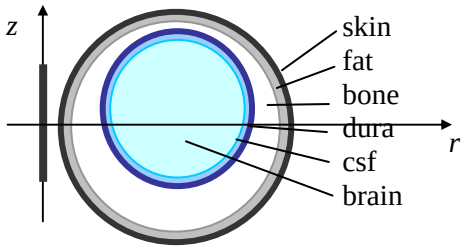

Fig. 3 Computational domain structure similar to [1] (layered eccentric 6-spheres model)

Table 1.
Characteristics of tissue subdomains [1]

TISSUE	Radius [mm]	Density [kg/m^3]	Conductivity [S/m]		Relative permittivity	
			900 [MHz]	1800 [MHz]	900 [MHz]	1800 [MHz]
skin	90	1100	0.87	1.18	41.4	38.9
fat	89.3	920	0.11	0.19	11.3	11
bone	87.7	1850	0.14	0.28	12.5	11.8
dura	67.2	1050	0.96	1.32	44.4	42.9
csf	66.7	1060	2.41	2.92	68.7	67.2
brain	64.7	1030	0.86	1.27	46.5	43.9

Two categories of global parameters (absorbed power and averaged *SAR* in each tissue) were computed and the results were compared with similar estimates presented in [1], based on an analytical computational technique. Table 2 shows the power absorbed in each tissue, as a percentage of the total power absorbed in the head and table 3 shows the averaged *SAR* in each tissue divided by the total absorbed power. The values were computed for two EMF frequencies (900 MHz and 1800 MHz); the dipole antenna is located at a distance of 10 cm at the side of the head. The reference data are taken from graphs in Figs. 4a and 5a, in paper [1].

Table 2
Power absorbed in each tissue as a percentage of the total absorbed power $100\,P / P_{total}$ [%]

$100\frac{P}{P_{total}}$ [%]	900 [MHz]		1800 [MHz]	
	paper [1] model	**2D FEM model**	paper [1] model	**2D FEM model**
skin	9	**9.37**	9	**8.7**
fat	3	**2.75**	3	**2.68**
bone	30	**31.38**	48	**50.25**
dura	2	**1.3**	2	**1.14**
csf	12	**11.89**	10	**9.48**
brain	43	**43.3**	28	**27.7**

Table 3
Averaged SAR in each tissue divided by the total absorbed power SAR / P_{total} [W/kg per W]

$\frac{SAR}{P_{total}}$ [$\frac{W/kg}{W}$]	900 [MHz]		1800 [MHz]	
	paper [1] model	**2D FEM model**	paper [1] model	**2D FEM model**
skin	0.168	**0.163**	0.112	**0.112**
fat	0.026	**0.025**	0.023	**0.024**
bone	0.015	**0.013**	0.016	**0.021**
dura	0.059	**0.044**	0.037	**0.037**
csf	0.143	**0.103**	0.081	**0.078**
brain	0.049	**0.024**	0.023	**0.015**

Test model nr. 2 has a circular multilayered structure, with only three different tissues: skin, bone and brain. The 2D axisymmetric computational domain looks similar to the cross-section of the spherical domain described in [4] (fig. 4). Table 4 gives the values of the electric properties, mass densities and dimensions for the subdomains.

Four categories of parameters (maximum local *SAR*, maximum *SAR* averaged over 1g, respectively 10 g of tissue and the absorbed power in the head) were computed. The estimates were performed on the three-layers heterogeneous structure (fig. 4) and on a homogeneous sphere, 100 mm radius, consisting of brain tissue. The antenna is located at a distance of 5 mm at the side of the head and radiates 125 mW. Paper [4] presents the results produced with two computational techniques: the method of moments (MoM) and the finite difference time domain technique (FDTD). The comparison of results is displayed in table 5.

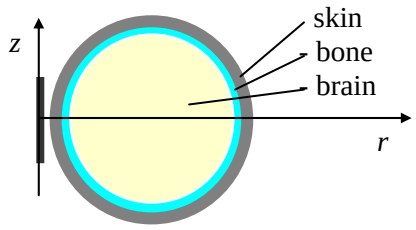

Fig. 4 Computational domain structure similar to [4] (layered concentric 3-spheres model)

Table 4.
Characteristics of tissue subdomains [4], at 1710 MHz

TISSUE	Radius [mm]	Density [kg/m^3]	Conductivity [S/m]	Relative permittivity
skin	100	1100	0.941	38.2
bone	95	1200	0.285	12
brain	90	1050	1.521	51.8

Table 5
Peak SAR values and absorbed power in homogeneous and 3-layers heterogeneous domains, at 1710 MHz

	local SAR $_{max}$ [W/kg]			1g avgd. SAR $_{max}$ [W/kg]			10g avgd. SAR $_{max}$ [W/kg]			Absorbed power [mW]		
	paper [4]		**2D FEM model**	paper [4]		**2D FEM model**	paper [4]		**2D FEM model**	paper [4]		**2D FEM model**
	MoM	FDTD		MoM	FDTD		MoM	FDTD		MoM	FDTD	
3-layered heterogeneous domain	8.19	8.54	**8.7**	3.41	3.72	**3.8**	2.21	2.34	**2.5**	107.5	106.14	**100.99**
homogeneous domain	11.8	11.31	**9.5**	5.64	5.35	**4.5**	2.62	2.88	**2.5**	100	101.9	**101.06**

A fairly good agreement could be observed for the compared data and the discrepancies are explained by the main difference between the models: in both situations a 2D FEM and a 3D analytical or numerical model are compared. The 2D FEM models, based on axial symmetry, are not derived from a realistic anatomy. However, they represent very useful and economic tools in modeling cross-sections of a 3D spherical body, particularly in dosimetry problems, for example in checking the compliance with exposure guidelines, when the order of magnitude of the EMF parameters is evaluated. Even in such simplified conditions, the computation proves to be at least as accurate as experimental testing.

Paper [7] demonstrates that the EMF distribution inside the exposed head is sensible to the external shape of the head: a larger curvature of the domain surface leads to lower inside electric field strength. For that reason we selected the ellipsoidal rather than the spherical shape, which models the head closely to the real shape.

RESULTS AND DISCUSSIONS

A study of the induced electric field strength *E* and *SAR* distributions is conducted with the **2D FEM model** (geometry from fig. 1.b with dielectric properties from table 1). First, a comparison is presented, between the SAR distributions inside the head when the EMF source is the half-wavelength dipole antenna, respectively the quarter-wavelength monopole antenna, at the same emitted power. The model is further used to estimate equivalent dielectric properties for reduced (equivalent) anatomical structures. The equivalent properties could be helpful for the design of experimental phantoms and 3D FEM models. Finally, an evaluation of uncertainties introduced in EMF parameters estimate by the use of several 2D FEM models is performed. The models present different inner structures and the source of MW is the dipole antenna.

SAR distribution inside the head exposed in the near field of the MW antenna

The head model is exposed in the near field of a mobile telephone antenna, radiating 125 mW, from the distance of 5 mm, at either 0.9 GHz and 1.8 GHz. To types of antennas were considered: a half-wavelength dipole antenna and a quarter-wavelength monopole antenna, accorded to the mentioned frequencies. Each time, the boundary condition for the EMF source is adjusted in order to maintain the same emitted power (125 mW). Figs. 5.a and 5.b present, for comparison, the Specific energy Absorption Rate, *SAR* spectra in the specified conditions. Local maximum values, $SAR_{\max}$ and maximum values averaged over a volume corresponding to 1g of tissue, $SAR_{\max\ 1g}$ and to 10g of tissue, $SAR_{\max\ 10g}$ are displayed for checking the compliance with exposure standards. The maximum values are higher for the monopole antenna, because the exposure is more focused than for the dipole antenna. As expected, the energy deposited in the tissues is higher at 1.8 GHz than at 0.9 GHz.

Equivalent dielectric properties for reduced head structures

The head structure presented in fig. 1 could be reduced to a more simplified model, having the same external shape and dimensions and an inner homogeneous structure. The electric properties of the reduced model (σ_{equiv} respectively ε_{equiv}) are computed with the FEMLAB software, by energy based equivalence, considering that the total absorbed power and total electric energy have the same values in the heterogeneous (composed by *i* different subdomaines) and equivalent homogeneous models:

$$\int_i \sigma_i (E_i)^2 \, \mathrm{dv} = \sigma_{equiv} \int_i (E_i)^2 \, \mathrm{dv}, \qquad \int_i \frac{1}{2} \varepsilon_i (E_i)^2 \, \mathrm{dv} = \frac{1}{2} \varepsilon_{equiv} \int_i (E_i)^2 \, \mathrm{dv}. \tag{5}$$

The method is applied to compute the equivalent dielectric properties of two reduced head models:

(1) reduced heterogeneous model with two subdomaines: equivalent **skull** (skin+fat+bone) and equivalent **brain** (dura+csf+brain);

(2) reduced homogeneous model: equivalent **head** tissue .

Fig. 6 presents the frequency dependence of the equivalent electric conductivity and dielectric permittivity, in the frequency range used in the GSM European system. The equivalent dielectric properties have the same values when computed either with the dipole antenna or the monopole antenna as the EMF source.

The equivalent properties facilitate a quantitative correspondence between numerical models and physical models (phantoms) used in measurements for microwave macroscopic dosimetry assessment. The results are promising for the opportunity of the simplified 2D model extension to a 3D one, with an optimized shape and internal structure.

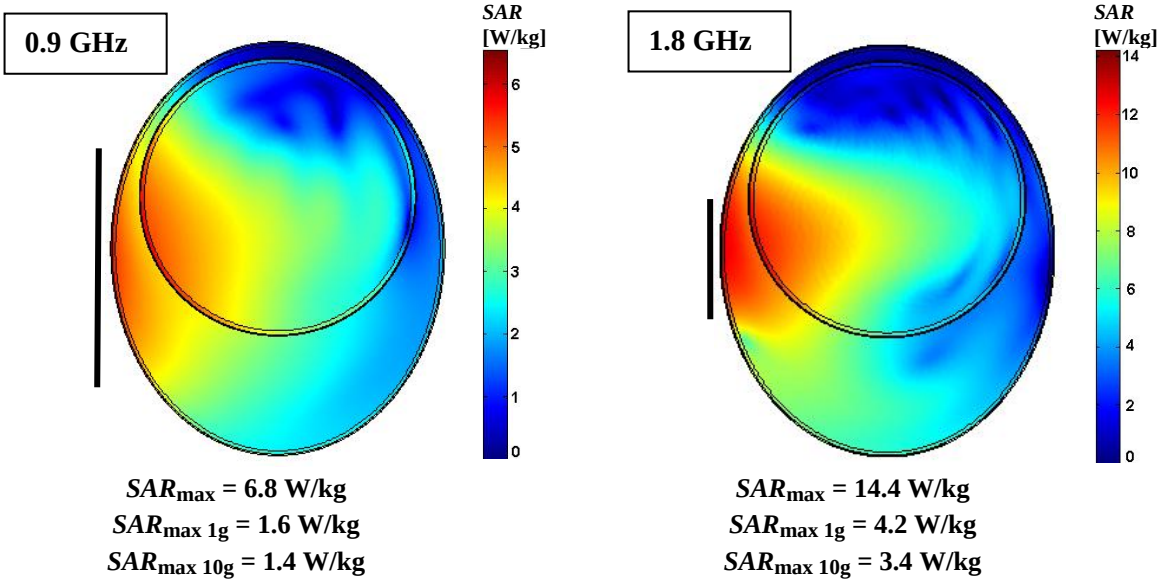

SAR_{max} = 6.8 W/kg
$SAR_{max\ 1g}$ = 1.6 W/kg
$SAR_{max\ 10g}$ = 1.4 W/kg

SAR_{max} = 14.4 W/kg
$SAR_{max\ 1g}$ = 4.2 W/kg
$SAR_{max\ 10g}$ = 3.4 W/kg

a. exposure to the half-wavelength center-fed dipole antenna

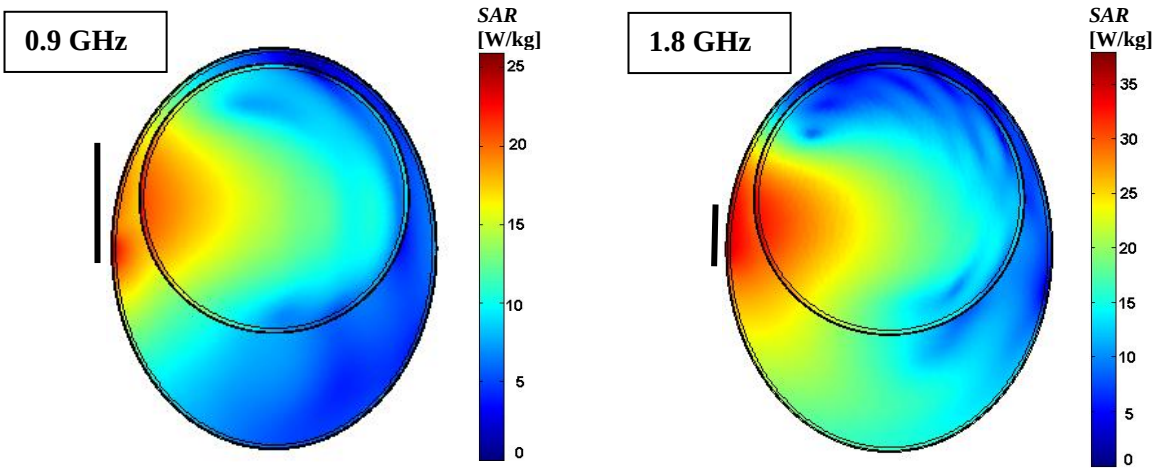

SAR_{max} = 25.9 W/kg
$SAR_{max\ 1g}$ = 6.5 W/kg
$SAR_{max\ 10g}$ = 5.1 W/kg

SAR_{max} = 38 W/kg
$SAR_{max\ 1g}$ = 9.2 W/kg
$SAR_{max\ 10g}$ = 7.5 W/kg

a. exposure to the quarter-wavelength monopole antenna fed at the base

Fig. 5 *SAR* spectra and characteristic values (SAR_{max}, $SAR_{max\ 1g}$ and $SAR_{max\ 10g}$) for the exposure of the head in the near field of an antenna placed at 5 mm near the head and emitting 125 mW

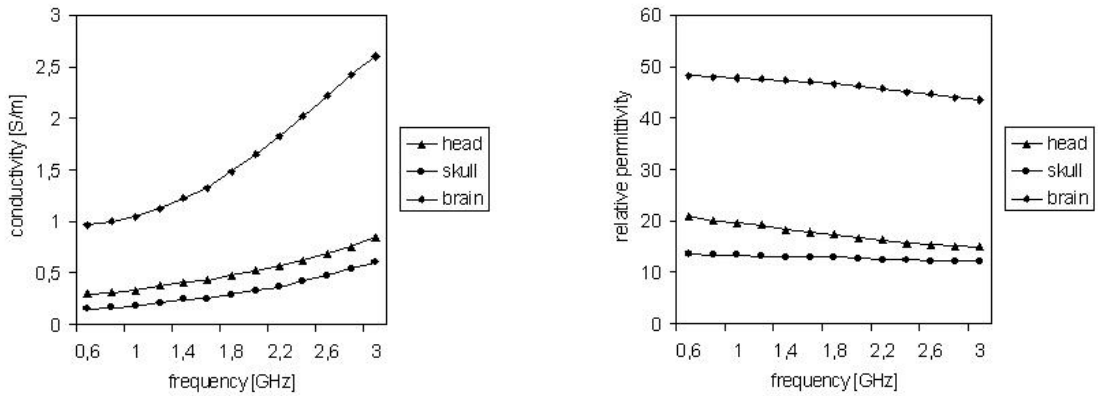

Fig. 6 Frequency dependence of the equivalent dielectric properties

EMF parameters estimate using 2D FEM models

Our study further investigates the uncertainties introduced in EMF parameters evaluation by the use of different 2D FEM models. We compare the *SAR* and *E* distributions inside the head exposed in the near field of the dipole antenna, at different frequencies, considering the following models:

(A) heterogeneous six layers model presented in figure 1
(B) reduced heterogeneous model with two sub-domains (skull and brain)
(C) reduced homogeneous model

The dielectric properties are presented above. In all cases the antenna is a half-wavelength dipole placed symmetrically at the left side of the head at the distance of 5 mm.

Electric field penetration in the exposed head (rms values) is presented for the models *(A-C)* in fig. 7, at the main frequencies in the MW considered range (0.9 GHz, 1.8 GHz and 2.5 GHz). Due to the position of the antenna, the *E* values on the (*Or*) axis are the highest in the domain. The results presented in fig. 7 support the good agreement among equivalent models (especially the heterogeneous ones, *A* and *B*). This is a good reason to use the values determined for equivalent dielectric properties in the design of 3D FEM models for the human head.

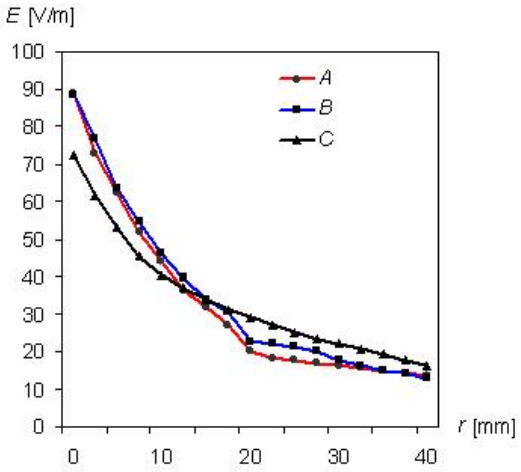

a. at 0.9 GHz

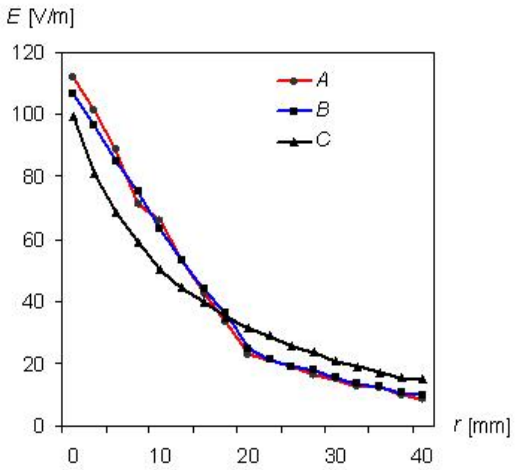

b. at 1.8 GHz

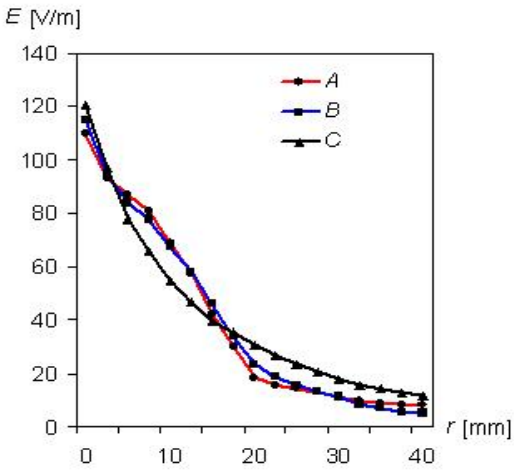

c. at 2.5 GHz

Fig. 7 *E* distribution (rms values) versus distance *r*, measured from the surface of the skin, for 2D FEM models

In a 3D numerical model, the degree of heterogeneity is crucial for the complexity of the model and computational resources; thin layers (like skin, fat, dura and csf) should be covered with a very dense FEM mesh. Consequently, any possibility to simplify the structure is appreciated.

The reduced heterogeneous structure (model *B*) proves to achieve the most desirable compromise between the accuracy of anatomical representation and the economy of computational resources. The uncertainty between *E*-field values computed for the

heterogeneous layered structure (model *A*) and for the reduced heterogeneous structure (model *B*) are in the limit of 10%, while for the reduced homogeneous structure (model *C*) the uncertainties go to 20%.

The *E*-field penetration depth was estimated for the three presented models (*A*, *B* and *C*), in the considered frequency range. Fig. 8 shows that the frequency dependence of the penetration depth for the heterogeneous model (*A*) and heterogeneous reduced model (*B*) are very similar, while the same function for the homogeneous model (*C*) has a noticeable different shape.

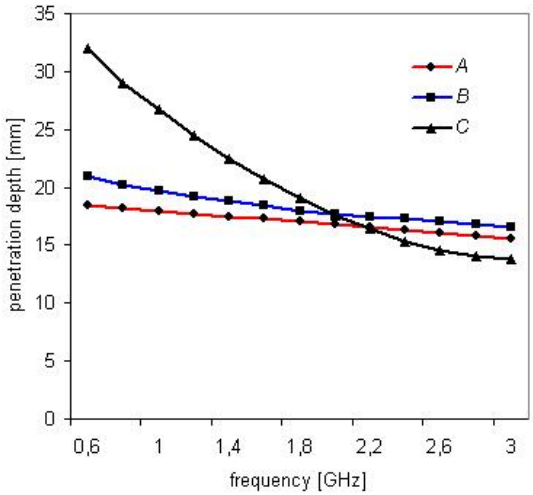

Fig. 8 Frequency dependence of the penetration depth, for 2D FEM models

CONCLUSIONS

The construction of the simplified 2D FEM model arise from the necessity to evaluate EMF parameters distribution in layered structures like anatomical tissues when exposed to MW either in day-to-day activities (as mobile phone use) or in medical therapy (hyperthermia, stimulation, etc.). Compared with more sophisticated models, the 2D FEM model demonstrates its advantages in economy of resources, accessibility and rapidity, while the results are sufficiently accurate for global estimates and for comparison with experimental *SAR* and *E* distributions from measurements on phantom human models. The results presented here are specific for the conditions related to mobile phone use near the head, but the method of equivalence between the heterogeneous anatomical structures and the homogeneous equivalent domains could be also applied to other parts of the body. The results are useful for the optimal design of 3D models..

We have proposed a quantitative correspondence between numerical models and physical models (phantoms) used in measurements for microwave macroscopic dosimetry assessment. In the evaluation of EMF penetration in tissue exposed to microwaves the *E* and *SAR* distributions were determined. Our results show that the inner distribution of the electric field has a low sensitivity to the dispersion of dielectric properties (in reasonable limits usual for practical situations) and to the heterogeneity level of the anatomical structure. In numerical and experimental modeling of human body exposure to ELF in the MW range it is important to reproduce the external shape of the body, but the models could be simplified in their inner structure.

The work presented here is part of a larger study, under the CNCSIS research grants nr.469/ 2003-2004.

References

[1] Moneda A. P., Ioannidou M. P., Chrissoulidis D. P. – "Radio-Wave Exposure of the Human Head: Analytical Study Based on a Versatile Eccentric Spheres Model Including a Brain Core and a Pair of Eyeballs", *IEEE Trans. Biomed. Eng*., vol. BME-50, pp. 667- 676, 2003

[2] Lin J. C., Gandhi O. P. – "Computational Methods for Predicting Field Intensities", Chapter 9, pp. 337-402 in *Handbook of Biological Effects of Electromagnetic Fields*, 2nd Edition, C. Polk and E. Postow, editors, CRC Press, Inc., Boca Raton, FL., 2000

[3] Christ A., Chavannes N., Pokovic C. K., Gerber H., Kuster N. – "Numerical and Experimental Comparison of Human Head Models for SAR Assessment", Foundation for Research on Information Technologies in Society, Swiss Federal Institute of Technology Zurich, Schmid & Partner Engineering AG, Zurich, 2002

[4] Koulouridis S., Nikita K. – "Characteristics of Power Absorption in Human Head Models Exposed to Normal Mode Helical Antennas", the 2nd Intl. Workshop on Biological Effects of Electromagnetic Fields, Rhodes, Greece, 2002

[5] Jin-Fa Lee – "Finite Element Methods for Microwave Engineering", ElectroScience Lab., EE Dept., The Ohio State University, 2002.

[6] Morega M., Machedon A. – "Specific Conditions for EMF Modeling in Human Exposure From Mobile Phone Technology", *Advanced Topics in Electrical Engineering ATEE-2002*, Bucharest, 2002

[7] Mihaela Morega, Alina Machedon, Stefan Samfirescu - "Dielectric Properties in Numerical Models of Biological Tissues for Applications in Microwave Dosimetry", *4th International Workshopon Materials for Electrotechnics, MMDE - 2004*, paper D – O2 – D04, Bucharest, Romania, 2004

[8] Andrei Negoias, Alina Machedon, Mihaela Morega – "Evaluation of Dosimetric Parameters in Biological Tissues Exposed to Microwaves", *4th European Symposium on Biomedical Engineering* , Patras, Greece, 2004.

[9] Mihaela Morega, Alina Machedon - "Dielectric Equivalent Properties for Nonhomogeneous Anatomical Structures", *1st International Conference on Biomaterials and Medical Devices, BIOMMEDD - 2004*, Bucharest, Romania, 2004

[10] Gabriel C., Gabriel S. - "Dielectric Properties of Body Tissues at RF and Microwave Frequencies", Report for Armstrong Laboratory (AFMC), Occupational and Environmental Health Directorate - Radiofrequency Radiation Division, USA, 2002

[11] FEMLAB 2.3b, User's Guide and Electromagnetics Module, COMSOL AB., 2003